Research Square

Preprints are preliminary reports that have not undergone peer review.
They should not be considered conclusive, used to inform clinical practice,
or referenced by the media as validated information.

Microbial diversity and insights into feeding behavior of the two-spot cotton leaf hopper (Amrasca biguttula)

Saptarshi Ghosh
University of Georgia
Vamsidhar Reddy Netla
University of Georgia
Uday Suresh
University of Georgia
Kamran Rashid
University of Georgia
Gulshan Kumar
University of Georgia
Jeffrey A. Davis
Louisiana State University
Rajagopalbabu Srinivasan
babusri@uga.edu

University of Georgia

Research Article

Keywords: leafhopper, cotton, symbionts, Wolbachia, Adintovirus, mesophyll, EPG, hopperburn

Posted Date: November 12th, 2026

DOI: https://doi.org/10.21203/rs.3.rs-10975063/v1

License: This work is licensed under a Creative Commons Attribution 4.0 International License.
Read Full License

Additional Declarations: No competing interests reported.

Title: Microbial diversity and insights into feeding behavior of the two-spot cotton leaf hopper (*Amrasca biguttula*)

Authors

Saptarshi Ghosh[1], Vamsidhar Reddy Netla[1], Uday Suresh[1], Kamran Rashid1, Gulshan Kumar[1], Jeffrey A. Davis[2], Rajagopalbabu Srinivasan[1]*

[1]Department of Entomology, University of Georgia,1109 Experiment Street, Griffin, GA 30223

[2]Department of Entomology, Louisiana State University, 404 Life Sciences Building, Baton Rouge, LA 70803

*Corresponding author

Key words: leafhopper, cotton, symbionts, *Wolbachia*, Adintovirus, mesophyll, EPG, hopperburn

Abstract

Recent invasion of the two-spot cotton leaf hopper (TSCL) (*Amrasca biguttula*) into the U.S. now threatens row and vegetable crops as well as ornamentals. TSCL ecology and biology, including microbial diversity, are understudied. Insect-specific microbes could influence host biology and ecology including insect-plant interactions. Here, microbiota (bacteria and viruses) within TSCL along with its feeding behavior were characterized using high throughput sequencing, microscopy, and Electrical penetration graph (EPG). Results revealed low diversity of bacteria dominated by *Wolbachia* and confirmed the absence of obligate (primary) symbionts. Two distinct and differentially abundant *Wolbachia* strains (B-supergroup) were found co-infecting midgut tissues of 60% of TSCL tested. Virome analysis uncovered a diverse complex of at least eight dsDNA genomes (12-17 kb) of adintoviruses (*Eupolintoviridae*), but no RNA viruses commonly found in other leafhoppers were identified. The mesophyll feeding nature of TSCL was identified by observing chlorophyll derived autofluorescence in midguts and higher abundance of chloroplast transcripts (photosystem I, II, Rubisco, cytochrome b6 and ATP synthase complex) in TSCL (whole insects) compared with thrips and aphids. EPG recordings showed a cell-rupture style of feeding with differences between adults and nymphs. Lastly, consistent with its cell-rupturing feeding style, no evidence for the presence of plant-pathogenic bacteria or viruses that could induce hopperburn was found. These results overall provide insights into the microbial diversity and feeding pattern of TSCL and lay a foundation for future research.

Key message: This work characterizes the TSCL microbiome and its mesophyll feeding pattern. Results show that TSCL lacks any obligate bacterial symbiont but co-harbors two differentially abundant strains of *Wolbachia*. Results also prove leaf mesophyll as the primary feeding niche of TSCL with a cell-rupture probing pattern. The implications of absence of a primary symbiont and mesophyll rupture feeding are discussed in the context of hopper-burn. The findings of this study lay a foundation for future research on the biology, ecology, and management of this invasive pest.

Introduction:

Amrasca biguttula (Ishida), the two-spot cotton leafhopper (TSCL) (Cicadellidae, Auchenorhynca, Hemiptera), is a polyphagous sap sucking pest that causes severe economic losses to wide range of crops including cotton (1), vegetables (2, 3) and ornamentals (4, 5). Originally native to Asia, TSCL was first detected in the USA in 2023 in Puerto Rico (6). By July 2025, it had spread to a majority of Southern States ranging from Texas to Virginia (7). Based on sequencing data, it appears that a single haplotype of TSCL is responsible for the invasion, and the same haplotype also is the most widespread globally (8). Factors driving the spread of this invasive haplotype in the USA are yet to be understood.

Hemipteran insects rely on obligate (primary) endosymbiotic bacteria to complement their nutritionally deficient phloem/xylem diets (9, 10). These symbionts compensate for nutritional imbalances and allow for diversification of insect species by facilitating or restricting access to new feeding niches (11). Cicadellidae members commonly harbor a primary bacterial symbiont, *Candidatus* Sulcia muelleri along with a companion symbiont, *Candidatus* Nasuia deltacephalinicola in specialized cells called bacteriocytes (12, 13). Occasionally, *Sulcia* is lost and replaced with other bacterial or fungal symbionts in cicadellids that have transitioned to phloem and/or parenchyma diets (14).

Other than obligate symbionts, cicadellids also harbor secondary symbiotic/facultative bacteria (15, 16) in bacteriocytes or other tissue such as fat bodies, midgut, or reproductive organs (17, 18). The role of secondary symbionts in cicadellids is yet to be fully understood. However, in other hemipterans they confer fitness benefits (19) and aid in defense against abiotic (20) and biotic (21–23) stress. In contrast, they also can confer negative impacts on host fitness by competing for resources (24, 25). Secondary endosymbionts are primarily maintained through vertical transmission but evidence for horizontal spread also exists (26–28). Other than direct influence on insect nutrition, abiotic/biotic stress defense, and developmental processes, bacterial symbionts can indirectly influence insect invasiveness by broadening their host range, mitigating host defense, and enhancing insecticide resistance (29–31).

The two-spot cotton leafhopper (TSCL) belongs to *Typhlocybinae* –the second largest subfamily within *Cicadellidae* (32), which differ from other leaf hoppers due to their use of mesophyll as the

primary feeding niche instead of the vascular tissue (32–34). Absence of any primary bacterial symbiont differentiates *Typhlocybinae* members from other leaf hoppers, and the absence is, in part, attributed to their nutrient rich mesophyll diet (17, 35). Potato leafhopper (*Empoasca fabae*) is the only known *Typhlocybinae* exception that harbors *Sulcia* –the primary symbiont (36).

Characterization of microbial diversity within TSCL and its feeding biology is necessary to reaffirm the relationship between nutrition and symbionts. Moreover, elucidation of microbial diversity within TSCL is important for understanding factors driving its spread across continents and haplotype divergence. This study assessed the microbiota (bacteria fungi and viruses) within TSCL by high throughput sequencing. In addition, probing and feeding patterns were characterized using high throughput sequencing, microscopy, and electrical penetration graph (EPG) technique. Lastly, this study examined the presence of TSCL-transmitted plant pathogenic bacteria and/or viruses.

Materials and Methods

Collection and maintenance of TSCL colony:

A laboratory population of *A. biguttula* was maintained for a minimum of four generations since field collection (adults; N~25) in September 2025 from cotton and eggplant at UGA Plant Sciences farm, Tifton, GA. The TSCL colony was maintained on cotton plants cv. PHY 339 WRF (Corteva, Indianapolis, IN, USA) in insect-proof cages (47.5 x 47.5 x 93 cm^3 BugDorm-4E4590 insect rearing cages, Megaview Science Co. Taichung, Taiwan) in a greenhouse at the University of Georgia, Griffin, GA at 27 ± 5 °C, 60% RH, and 14 h L:10 h D photoperiod.

Microbiome analyses

Bacteria diversity: High throughput amplicon sequencing of the variable region (V3-V4 region) and full length 16S rDNA was performed for identification of bacteria within TSCL. Identified sequence variants of bacteria were verified by restriction fragment length polymorphism (RFLP) of PCR amplified full length 16S rDNA using generic primers. Bacteria diversity within symptomatic TSCL-infested plant samples also was investigated by amplicon sequencing of 16S rDNA (V3-V4) to identify the presence of any TSCL-transmitted plant pathogenic bacteria/phytoplasmas.

Amplicon sequencing of V3-V4 region of 16S rDNA:

V3-V4 region (450 bp) of 16S rDNA was amplicon sequenced (250 bp paired end reads) from genomic DNA samples (N=2) extracted from the laboratory TSCL (10 adults each) population reared on cotton. V3-V4 region was PCR amplified using barcode-tagged primers (Table S1) and sequenced on Illumina Novaseq 6000 sequencing platform (Illumina, San Diego, CA, USA) following the metagenomic amplicon sequencing service pipeline at Novogene Corporation Inc. (Sacramento, CA).

Bioinformatic analyses were carried out using the QIIME2 v2025.4 (quantitative insights into microbial ecology) platform (37). Adapters and primers were removed from paired end reads using QIIME2 plug in q2-cutadapt (37). Cleaned reads were quality filtered, dereplicated, and chimeras were removed and merged using QIIME2 plug in dada2 (qiime dada2 denoise-paired) to obtain amplicon sequence variants (ASVs). ASVs were classified using the Qiime2 Naïve Bayesian classifier against SILVA 16s/18s SSU database (SILVA release 138.2). ASVs matching chloroplast and mitochondria were not considered for downstream analyses. Identified ASVs from TSCL were compared with publicly available data of other *Wolbachia* containing *Typhlocybinae* members (*Fagocyba cruenta*, *Kybos virgator, Linnavuoriana sexmaculata, Notus flavipennis, Zygina hyperici* and *Zygina rubrovittata*) (17). ASVs of TSCL and other *Typhlocybinae* members were rarefied to sample depth of 79,907 and used for beta diversity Bray-Curtis dissimilarity analysis. Beta diversity analyses with Bray-Curtis dissimilarities were performed using QIIME2 diversity plug in core-metrics-phylogenetics. Principal coordinate analysis (PCoA) plot with beta diversity Bray-Curtis distances plots were generated using R packages and scripts (38). The statistical difference of beta diversity was performed with permutational multivariate analysis of variance (PERMANOVA) with Mann-Whitney U test.

Bacteria diversity within field collected leaf samples showing puckering and distortion symptoms from cotton (N=4), eggplant (N=2) and okra (N=2) plants infested with TSCL also were analyzed using the V3-V4 amplicon sequencing pipeline. Leaves from respective plant species without insect infestation were used as control.

Amplicon sequencing of full length 16S rDNA: Genomic DNA samples (N=2) extracted from TSCL (10 adults each sample) were used as template for amplicon sequencing of complete 16S

rDNA using metagenomic sequencing services at Novogene Corporation Inc. (Sacramento, CA). Near full-length 16S rDNA was PCR amplified using barcoded adapter primers (Table S1), purified, and pooled in equimolar amounts prior to library preparation using Kinnex long-read sequencing technology. Libraries meeting quality standards were sequenced on the PacBio Revio platform using Single Molecule, Real-Time (SMRT) sequencing to obtain high-quality long reads.

Raw PacBio HiFi reads were processed using the DADA2 plugin within the QIIME2 pipeline (qiime dada2 denoise-ccs). This workflow included denoising, which encompassed quality filtering, dereplication, and chimera removal to identify ASVs. Taxonomic assignment of the identified ASVs was deduced using a Naïve Bayesian classifier trained against SILVA 138.2 (16S/18S) rDNA database. The classified ASVs and resulting feature tables were subsequently utilized for downstream diversity and phylogenetic analyses.

Validation of *Wolbachia* isolates by PCR-RFLP of full length 16S rDNA and partial Wolbachia surface protein (Wsp) gene: DNA extracted from pooled samples (N=10) was used as template to amplify a 1.5 kb fragment of eubacterial 16S rDNA using universal primers (39) and partial Wsp *Wolbachia* gene fragment using 81F and 471R primers (Table S1). The PCR fragments were ligated to pJET1.2/blunt cloning vector (ThermoFisher Scientific), transformed to *E. coli,* and positive bacterial colonies with inserts were confirmed by PCR using pJET1.2 forward and reverse sequencing primers. Positive colonies for 16S rDNA (N=70) and Wsp (N=40) were screened by RFLP using *Taq*I and *Alu*I restriction enzymes, respectively, as previously described (39). Plasmids extracted from a minimum of three clones showing unique RFLP profiles were Sanger sequenced in both directions using pJET forward and reverse sequencing primers and analyzed for nucleotide differences.

Amplicon sequencing of full length fungal ITS: Fungal diversity within TSCL samples was captured by amplicon sequencing of the complete ITS region using amplicon metagenomic sequencing services at Novogene Corporation Inc. (Sacramento, CA). Universal primers (Table S1) with barcoded adapter primers were used to amplify complete ITS and sequenced on the PacBio Revio platform using Single Molecule, Real-Time (SMRT) sequencing. Raw PacBio HiFi reads were processed using the DADA2 plugin within the QIIME2 pipeline (qiime dada2 denoise-ccs), as described above.

PCR based detection of *Wolbachia,* quantitation of sequence variants, and phylogeny: To determine the frequency of TSCL harboring *Wolbachia*, DNA extracts from individual adults (40) were screened for the presence of *Wolbachia* by PCR using 16S rDNA specific primers (Table S1). *Wolbachia* sequence variants, WSV1 and WV2 were detected and quantitated within individual TSCL samples by qPCR using specific primers (Table S1). Relative quantities of WSV1 and WSV2, normalized to the ribosomal protein S13 (RPS13) gene (Table S1), were calculated using the ΔΔct method. Significant differences were inferred using Wilcoxon's rank sum test.

Nucleotide sequences of 16S rDNA and wsp and *ftsz* genes of *Wolbachia* obtained from laboratory TSCL were aligned with sequences from other arthropods available in GenBank. The best-fit nucleotide substitution model was identified according to Bayesian Information Criterion score (BIC), and phylogenetic trees were constructed using maximum likelihood with 1000 bootstrap replicates using IQ-TREE v3.1.0 (41). The resulting consensus trees were visualized using iTOL v7 (Interactive Tree of Life) (42).

Localization of *Wolbachia* within TSCL and midgut tissues: *Wolbachia* within whole TSCL adults were localized by fluorescent *in situ* hybridization (FISH) using a cyanine 3 labeled *Wolbachia* specific DNA probe (Table S1) or without probe (control) as previously described (43). Briefly, whole insects were fixed in Carnoy's fixative (chloroform: ethanol: glacial acetic acid, 6:3:1, v/v) overnight, cleared with 6% hydrogen peroxide in ethanol, and incubated at room temperature with probe (100 nM) in hybridization buffer (20 mM Tris pH 8, 0.9 M NaCl, 0.01% SDS, 30% formamide). Samples were mounted on slides with hybridization buffer containing 100 µg/ml DAPI and viewed under Zeiss LSM700 confocal laser scanning microscope. *Wolbachia* was immunolocalized within fixed (4% paraformaldehyde) TSCL midgut tissues using of *Wolbachia* FtsZ polyclonal antibody (2 µg/ml) (ThermoFisher Scientific) and Alexa Fluor™ 488 conjugated goat-anti-rabbit secondary antibody (4 µg/ml) as described earlier (44). Midgut samples stained only with the secondary antibody were used as control. Mounted midgut samples were viewed using a Zeiss LSM700 confocal laser scanning microscope.

RNA sequencing of TSCL and host plants for RNA virus discovery

Leaf samples from field grown (UGA plant sciences farm, Tifton, GA) cotton, eggplant and okra infested with TSCL showing puckering and distortion symptoms, and laboratory-reared TSCL

adults and cotton plants for rearing them, were collected and processed for identification of prospective TSCL-transmitted plant viruses. Total RNA from TSCL and plant samples were extracted using RNeasy micro kit (Qiagen, GmbH, Hilden, Germany) and Spectrum Plant Total RNA Kit (Sigma-Aldrich Inc. St. Louis, MO, USA), respectively. Extracted RNA was treated with Ribo-zero rRNA removal kit (Illumina, San Diego, CA, USA) for ribosomal RNA (rRNA) depletion and used for cDNA library preparation using random hexamers. The libraries were then sequenced using Illumina Novaseq X Plus platform (Novogene Corporation Inc. Sacramento, CA, USA).

Raw reads were quality controlled using FastQC v0.12.0 (45) and MultiQC v1.28 (46), and adapters were removed and trimmed using fastp v0.23.4. Processed reads were assembled into contigs using either reference-based or *de novo* assembly. Virus reads were enriched by removal of host reads by mapping total reads to respective reference genomes. Reads from cotton and okra were mapped to their available respective reference genomes (cotton: GCF_007990345.1, okra: GCA_035048815.1) from NCBI. Unmapped reads were extracted using bowtie2 v2.5.4 with default parameters and assembled into contigs using *de novo* assembler SPAdes v4.1.0 (47) with the rnaviralSPAdes parameter and K-mers of 21,33,55 and 77.

For TSCL and eggplant, total trimmed reads were *de novo* assembled into contigs using SPAdes v4.1.0 (47) with the rnaviralSPAdes parameter and K-mers of 21,33,55 and77 due to the unavailability of a reference genome. Assembled contigs were analyzed by BLASTX algorithm search against non-redundant (nr) virus protein database in DIAMOND v2.1.15 (48). Open reading frames (ORFs) were identified from assembled virus contigs using the NCBI ORF finder algorithm. Translated proteins from the ORFs were compared with other virus proteins in the non-redundant protein database by BLASTP and with predicted virus domains using NCBI conserved domain database (CDD) and HHpred search. The virus contigs were mapped back to raw reads using Bowtie2 v2.5.4 to check read abundance and depth.

Comparison of autofluorescence from chloroplast pigments in midguts:

To assess mesophyll tissue feeding, TSCL adults reared on cotton plants were either provided with a 48-hour feeding access on an artificial diet (15% sucrose) to clear guts or were clip-caged (48 hours) to an excised cotton leaf with petiole dipped in water. Next, midguts from diet or leaf-fed

insects were extracted in 1X PBS and then fixed for 45 minutes with 4% paraformaldehyde, washed thrice with PBST (1XPBS + 0.05% Tween 20), and mounted with PBS containing DAPI (100 µg/ml) on glass slides with coverslips. Midguts from leaf- and diet-fed insects were visualized under Fein-Optic FZ8 stereo-trinocular microscope and photographed to compare chlorophyll derived green pigmentation. Green autofluorescence between the leaf- and diet-fed midgut samples were compared using a Zeiss LSM700 confocal laser scanning microscope using 555 nm excitation and 583 nm emission.

Comparison of chloroplast transcripts in RNA-seq libraries of TSCL with other phloem feeders:

Abundance of chloroplast specific transcripts of TSCL with other phloem feeding insect pests of cotton were compared to examine mesophyll feeding. RNA-seq reads of TSCL generated in this study and RNA-seq datasets from cotton-reared Western flower thrips, *Frankliniella occidentalis* (epidermal feeder) (unpublished), and cotton aphid, *Aphis gossypii* (phloem feeder) (49) generated previously, were compared for abundance of chloroplast specific transcripts. Processed reads were mapped to the cotton reference genome (*Gossypium hirsutum* L.: GCF_007990345.1) using splice aware STAR RNA-seq aligner (50). Mapped reads were assembled and annotated using a reference-guided approach in StringTie (51) by utilizing the cotton reference genome as a scaffold. The resulting transcripts were compared and consolidated against the reference annotation using Gffcompare to ensure structural accuracy. Transcript abundance for chloroplast-related genes was subsequently quantitated using StringTie, with expression levels normalized as transcripts per million (TPM) to facilitate downstream comparative analysis.

Electrical penetration graph (EPG) recordings: TSCL adults (1-10 days old) and nymphs (4-5th instar) were attached to 3.5 cm long and 12 µM diameter gold wire (0.0005-inch diameter, Sigmund Cohn Co. Mount Vernon, NY, USA) using water-based silver glue (https://www.epgsystems.eu/files/SILVER%20GLUE%20recipe.pdf) following protocols outlined in Walker et. al 2022 (52). Post wiring, insects were starved for one hour and placed on abaxial surface of the topmost fully expanded leaf of a cotton plant cv. PHY 339 WRF (4-5 leaf stage). EPG waveforms were recorded for 10 hours using a 4-channel AC/DC EPG monitor (EPG Technologies, Gainesville, FL, USA) at one TSCL per channel using the DI-710 USB data

acquisition system (Dataq Instruments, Akron, OH, USA) at 25-30 mV DC substate voltage, 75X gain, and 10^9 Ω input resistance.

Results:

Bacteria diversity in TSCL: Good's coverage (>99.99%) estimates of high-throughput sequencing of the 16S rDNA gene indicated that the sampling depth sufficiently captured total bacteria diversity and revealed that a low-diversity bacteria community overwhelmingly dominated by *Wolbachia* reside within TSCL. In both the V3-V4 dataset (254,802 amplicon sequences) and the full-length PacBio dataset (9,166 amplicon sequences), most reads belonged to *Wolbachia* (Fig. 1A, 1B; Table S2). Notably, no obligate bacterial symbiont (*Baumannia*, *Sulcia*, *Zinderia*, *Nasuia*) or other facultative endosymbionts commonly associated with *Cicadellidae* insects could be detected. Bacterial diversity structure compared using PERMANOVA analysis of 16S rDNA sequences showed no significant differences between TSCL and other *Typhlocybinae* members. TSCL bacterial community shared the closest taxonomic abundance with *Kybos virgator* —a leafhopper infesting willow trees in Poland (Fig. 1C). PCR screening of individual TSCL samples with *Wolbachia* specific 16S rDNA confirmed that only 60.0% (18/30) of individuals harbored *Wolbachia* (Fig. 1D), while the rest were devoid of any secondary symbiont.

Full-length 16S sequencing identified two *Wolbachia* sequence variants, designated as WSV1 and WSV2 in this study, with WSV1 being the dominant variant (71% of *Wolbachia* reads) (Fig. 2A, Table S2C). Presence of the two *Wolbachia* isolates was validated by PCR-RFLP of cloned full length 16S rDNA and *Wsp* partial gene fragment, which yielded unique profiles for the more abundant WSV1 and the less abundant WSV2 isolates. Notably, qPCR analysis using variant-specific primers targeting the *Wsp* gene confirmed that both isolates are co-harbored within TSCL individuals; albeit WSV1 was twice as abundant as WSV2 (Fig. 2B). Phylogenetic analysis of *Wolbachia* 16S rDNA, *Wsp*, and *FtsZ* nucleotide sequences generated in this study placed both WSV1 and WSV2 within the 'B' subgroup of *Wolbachia* (Fig. 3A, B, Fig. S1). The less abundant WSV2 isolate clustered closely with *Wolbachia* isolates previously identified from TSCL in Pakistan, whereas the dominant WSV1 formed a distinct clade (Fig. 3 A, B, S1).

Localization of *Wolbachia* within TSCL: FISH analysis on wholemount TSCL adults localized *Wolbachia* signals primarily in the midgut region (Fig. 3A), whereas no signal was detected from control insects without the probe (Fig. S2A). This was confirmed by immuno-histochemistry on dissected midguts of TSCL using *Wolbachia* FtsZ polyclonal antibody. Localization was observed in the conical midgut, midgut loop, and midgut posterior regions (Fig. 3 B, C) (N=4). No signal was detected from a subset (N=5) of midguts (Fig. S2B) thereby confirming the absence of *Wolbachia* in some individuals. No signal was observed in control midguts stained only with the secondary antibody.

Virus diversity in TSCL: BLASTX query of *de novo* assembled contigs from processed TSCL RNAseq reads against the non-redundant virus protein database yielded no detectable RNA viruses. Instead, 507 viral contigs with high similarity to dsDNA viruses belonging to the genus *Adintovirus* (*Eupolintoviridae*) were identified. From these, eight near full-length adintovirus genomes (12.9-17.3 kb), designated as TSCL adintovirus 1-8 were assembled (Fig.4). Reads of TSCL Adintovirus 7 were most abundant, followed by adintovirus 4 and 6 (Table S3A). Annotation of the genome using BLASTP, CDD, and HHpred algorithms revealed a characteristic genome organization of adintoviruses, comprising ORFs encoding for DNA polymerase type B (Pol B), IS481 transposase, Integrase, Filament temperature-sensitive mutant K (FtsK), Hexon, Penton, GasderminX, Cupiennin, Phospholipase A2-like domain (PLA2X), Adenain, Malestrom (MAEL), and Phage T7 tail fiber proteins (Fig. 4). Pairwise comparison of PolB amino acid sequences of the TSCL adintoviruses revealed that the abundant TSCL Adintovirus 7 belonged to betadintoviruses sharing 10.9% and 39.3% (Table S3B) identity with reference sequences of *Mayetiola barley midge adintovirus* (*Alphaadintovirus*, YP_010796961.1) and *Terrapene box turtle adintovirus* (*Betaadintovirus*, YP_010796957.1), respectively. The other seven viruses shared higher identity (>36%) with alphadintoviruses (Table S3B). The presence of two abundant alphadintoviruses (TSCL adintovirus 4 and 6) and the betadintovirus (TSCL adintovirus 7) was validated by PCR amplification from DNA samples extracted from individual TSCL adults (N=17) using PolB-and Hexon (major capsid protein) specific primers. All three adintoviruses screened in this study were detected from 100% of tested samples.

Fungal diversity: No symbiotic fungi were identified from TSCL samples.

Evidence of TSCL as mesophyll feeders:

Autofluorescence of midguts: Midguts dissected from leaf-fed insects were green at the conical midgut region (Fig. 4A) compared with midguts from diet-fed adults (Fig. 4B). Presence of the chlorophyll pigment was confirmed by autofluorescence detection from the conical midgut region (Fig. 4 C, D) of leaf-fed insects. Autofluorescence also was detected from the midgut loop region but not in the conical midgut region of control insects (Fig. 4 E, F), probably due to partial gut clearing and remnant chlorophyll pigments.

Comparison of host plant chloroplast transcripts between pests of cotton:

To further assess the mesophyll feeding nature of TSCL, normalized transcripts of cotton chloroplast genes identified from RNAseq data of TSCL, Western flower thrips (epidermal feeder), and cotton aphid (phloem feeder) were compared. A total of 49 different chloroplast genes were identified from TSCL, compared with 23 and 4 genes identified from thrips and the aphid, respectively (Fig. 7). Moreover, normalized transcript abundance of chloroplast marker genes belonging to photosystem I, II, Rubisco, cytochrome b6, and ATP synthase complex was higher in TSCL compared with thrips and the aphid (Fig. 7). These results reiterated that plant mesophyll could be the primary feeding niche for TSCL.

EPG recordings: Waveforms recorded for TSCL probing were consistent but produced distinct patterns for adults (N=7) and nymphs (N=5), respectively (Fig. 8 A, B). Both indicated cell rupture style of probing characterized by rapid ‘in-and-out’ stylet movement into plant cells. Wave patterns in nymphs were more frequent but of lower amplitudes compared with adults (Fig. 9, 10). Waveforms recorded for adults included a regular sequence of spikes (A1 and A2) but at much lower frequency than in the case of nymphs (Fig. 9, 10). The A1a and A1b waveforms were regular and smooth at the tip but the latter had higher amplitudes. The A2 waveforms contained ruffles and were pointed at the tips. A brief span of potential drops also was observed after A1 and A2 waveforms.

No evidence for TSCL transmitted pathogens causing hopperburn symptoms:

Analysis of symptomatic plant tissues did not implicate a TSCL-transmitted pathogen as the cause of "hopperburn." 16S rRNA sequencing revealed no known plant pathogenic bacteria,

phytoplasmas, or *Spiroplasmas,* in symptomatic leaves. The bacterial communities of TSCL and field/lab collected host plant samples were significantly different and clustered separately in PCoA analysis (Fig. S3). Similarly, RNA-seq analysis of symptomatic plants did not identify any viruses associated with TSCL infestation, though Cotton leaf roll dwarf virus (CLRDV) was incidentally detected in field-collected cotton.

Discussion:

Bacterial diversity: Leafhoppers belonging to *Typhlocybinae* sub-family exhibit low microbial diversity and in most cases are devoid of obligate/primary bacterial symbionts (17). Kobialka et al (17) identified *Wolbachia* as the predominant secondary bacterial symbiont within *Typhlocybinae* species. The results of this study showed that like other *Typhlocybinae* members, TSCL did not harbor any obligate bacterial or fungal symbionts, but *Wolbachia* was the predominant secondary bacterial symbiont. Reason for absence of obligate symbionts within this cicadellid sub-family remains unknown; however, their nutrient rich mesophyll diet could compensate for the lack of endosymbionts (17, 34). *Empoasca fabae*, another mesophyll feeding (33) *Typhlocybinae* pest of alfalfa, potato, and leguminous crops in the US, harbors *Sulcia* as a primary symbiont (36) alongside *Wolbachia* (53). Comparative studies of these two leafhopper species are imperative to understanding the impact of the absence of a primary symbiont on the host biology and feeding strategy.

This study revealed that *Wolbachia* is not fixed in the invading TSCL population screened in this study. It was only detected in 60% of the individuals. Similar *Wolbachia* incidences (61.5 %) were previously reported from TSCL populations in Pakistan (54). Genetically diverse strains of *Wolbachia* belonging to B supergroup are harbored within *Typhlocybinae* members, including TSCL (17, 35, 36, 54, 55). Phylogenetic analysis in this study confirmed that two different strains of *Wolbachia* with varying abundance co-infect the TSCL population screened in this study. Asymmetric densities of co-inhabiting *Wolbachia* variants are well-documented (56–58); however, factors accounting for the observed asymmetry remain unknown. Notably, the less abundant WSV2 strain clustered together with *Wolbachia* strains previously identified from TSCL populations from Pakistan. Whereas the more abundant WSV1 strain clustered differently. A recent study comparing phylogenetic relationships of global populations of TSCL using mitochondrial cytochrome oxidase markers revealed the dominance of a single haplotype across

native regions in South Asia and mainland USA (8). These findings reiterate the importance of studying microbial diversity together with insect genetic markers to understand the ecological history of insects.

Wolbachia drives its spread by manipulating reproduction of its insect host (59), and evidence of *Wolbachia* indued cytoplasmic incompatibility and feminization is well documented in leaf/plant hoppers (35, 55, 60, 61). Results from this study show that *Wolbachia* resides within midguts of TSCL and are similar to previous reports from other *Typhlocybinae* members (17, 36). Midgut residing *Wolbachia* may supplement vitamins (62), induce immune response (63), or stabilize the midgut environment (64); however, its exact role in TSCL biology needs to be elucidated.

Virus diversity: Virus diversity analysis of *Empoasca fabae* (65), *Matsumurasca onukii* (66) show predominance of RNA viruses belonging to *Iflaviridae*, *Solemoviridae*, *Lispiviridae*, *Phenuiviridae* and *Nidovirales*, and one DNA virus belonging to *Parvoviridae*. Recently Iflaviruses (+ve, ssRNA) have been identified from TSCL samples from India (67) and China (MZ367599.1). Surprisingly, no RNA virus could be detected within the TSCL samples analyzed in this study, but eight diverse full length dsDNA genomes (12-17 kb) of adintoviruses (TSCL Adintovirus 1-8) were identified from the RNAseq data. Adintoviruses were initially considered as polintons *aka* mavericks, which are large dsDNA transposons widespread among eukaryotic genomes and identified by the presence of genes encoding protein-primed type B DNA polymerase (PolB) and a retroviral-like integrase (68). However, recent characterization of double-jellyroll major capsid proteins (hexons), single-jellyroll minor capsid proteins (pentons), and virus genome packaging ATPases (FtsK) (68) have redefined as viruses belonging to a newly proposed family, *Adintoviridae* (69). Adintoviruses are further classified as alphadintoviruses and betadintoviruses, based on the identity of the PolB reference sequences (pfam03175) in CDD database. Results in this study show that out of the eight adintoviruses detected from TSCL, seven belonged to the genus *Alphadintovirus*, whereas the most abundant (TSCL adintovirus 7) belonged to the genus *Betadintovirus*. It is noteworthy that TSCL adintovirus 6 genome encodes characteristic beta-class accessory proteins such as gasderminX and cupiennin together with an alpha-group PolB, suggesting possible horizontal gene transfer between alpha and beta adintoviruses (69).

Adintoviruses can live a dual lifestyle of an endogenous virus element that can be induced to produce infectious virus particles (70). Interestingly, *Spodoptera* adintovirus genomes within *Sf*9 cells (a standard insect cell culture line) produced infectious virions that could infect High Five cells—another standard insect cell line (69). Whether TSCL adintoviruses live as endogenous viruses integrated within the host genome or can form infectious particles remains to be resolved. Even if adintoviruses only remain as long-term heritable endogenized elements, mapping its genetic diversity within global TSCL populations can shed light on the ecological and evolutionary history of its insect host (71).

Evidence for mesophyll feeding: This study demonstrates the mesophyll feeding nature of TSCL using microscopic evidence of higher chlorophyll derived autofluorescence in midguts extracted from leaf-fed adults compared with control midguts extracted from artificial diet-fed adults. The presence of higher numbers of chloroplast derived RNA transcripts within RNAseq data of TSCL compared with phloem/epidermal feeders further supports mesophyll feeding. In higher plants, mesophyll cells contain more and larger chloroplasts compared with epidermal or phloem parenchyma cells (72, 73). In this study, higher abundance of chloroplast transcripts identified in TSCL compared with thrips and the aphids reiterates its mesophyll feeding nature.

Mesophyll feeding *Typhlocybinae* members use rapid 'in-and-out' movement of their stylet to rupture plant cells and ingest cell contents (74, 75). This unique stylet movement along with secreted salivary effectors, induces plant wound responses leading to hopperburn symptoms (75). EPG patterns for TSCL adults and nymphs in this study clearly show similar stylet movement indicative of cell rupture feeding. Interestingly, distinct wave patterns were observed between adult and nymphs, with highly rapid low amplitude stylet movements seen in the case of nymphs than adults. This probing pattern by nymphs could be responsible for more pronounced foliar symptoms than adults (1, 2). Hunter et al. (33) described three different waveforms viz., I_a, I_b, and I_c of mesophyll feeding *Empoasca fabae* through EPG. High amplitude peaks (I_a) indicated lacerating stylet movement; I_b corresponded to single spongy mesophyll cell puncture and feeding; and I_c indicated ingestion activity. Although the exact plant tissue associated with ingestion (I_c) feeding was not determined, duration of I_c events has been implicated with mesophyll (< 2 min) or phloem feeding (>2 min) by the potato leafhopper. The waveforms A1 and A2 described in this study are very similar to the I_a and I_b waveforms described previously (33, 74, 76). However, no

clear I_c like waveform was identified from EPG recordings in this study. It is important to note that phloem restricted plant pathogens such as phytoplasmas (77, 78) and mastreviruses (79) have been detected from TSCL, thereby suggesting that TSCL also feeds on the phloem tissue. Thorough characterization of EPG waveforms described in this study together with microscopy is needed to decipher the extent of mesophyll and phloem feeding by TSCL. Nevertheless, TSCL feeding induced symptoms (Fig. S4) are likely a cumulative effect of its cell rupture feeding style and secreted salivary effectors. Experimental evidence confirming systemic effect of TSCL secreted saliva and functional characterization of salivary proteins is essential to understanding mechanisms associated with hopperburn symptoms.

Genbank accession numbers: Nucleotide sequences generated in this study have been deposited in NCBI Genbank under accession numbers PZ545711-17 (16S rDNA), PZ547707-12 (Wsp) and PZ547713 (FtsZ). Raw sequence reads generated in this study for amplicon sequencing of bacterial 16S rDNA of TSCL and host plants; fungal ITS; RNAseq of TSCL, host plants and thrips have been submitted to NCBI under the bioproject PRJNA1490287. TSCL adintovirus genomes have been submitted under the accession numbers PZ860860-67.

Funding acknowledgement: This work was partially supported by the USDA National Institute of Food and Agriculture Hatch project #GEO-00671from the Georgia Agricultural Experiment Station.

Figure Legends:

Fig. 1: Percentage composition of bacteria genera captured by V3-V4 segments (A) and full length (B) 16S rDNA amplicon sequencing. Principal co-ordinate analysis (PCoA) of Bray-Curtis dissimilarities showing bacterial community composition of TSCL and other *Wolbachia* harboring *Typhlocybinae* members (C). PCR screening for *Wolbachia* prevalence in individual TSCL adult samples (N=30) using 16S rDNA-specific primers (D).

Fig. 2: Percentage abundance of *Wolbachia* sequence variants identified by full length 16S rDNA amplicon sequencing (A) and relative quantitation of variants normalized to rps13 gene by qPCR (B).

Fig.3: Phylogenetic relationship between TSCL harbored *Wolbachia* and other *Wolbachia* strains based on aligned 405 bp of 16S rDNA (A) and 461 bp of *Wsp* (B) nucleotide sequences. Nucleotide substitution models HKY+F+G4 and TPM3u+F+G4 were used for 16S rDNA and Wsp, respectively. *Wolbachia* strains from *Typhlocybinae* members (17) are indicated in blue and sequence variants identified by amplicon sequencing and PCR-RFLP in this study are highlighted in red and yellow, respectively.

Fig. 4: TSCL adult wholemount showing *Wolbachia* (red) and DAPI stained nuclei (blue) in midguts using FISH with cyanine3 labelled *Wolbachia* specific DNA probes (A), and immuno-localization of *Wolbachia* (red) in midguts using *Wolbachia* FtsZ polyclonal antibody (B), and magnified (20x) area under inset (C). CM, ML, PM and MT denote conical midgut, midgut loop, posterior midgut, and Malpighian tubule, respectively.

Fig. 5: Genome organization of full-length *Adintovirus* genomes (*Adintovirus* 1-8) identified in this study. Predicted open reading frames (ORFs) are represented with their orientation and encode DNA polymerase B (Pol B), IS481 family transposase, retrovirus-like integrase, double-jellyroll major capsid protein (hexons), single-jellyroll minor capsid protein (pentons), filament temperature-sensitive mutant K (FtsK), gasderminX, cupiennin, Phospholipase A2-like domain (PLA2X), Adenain, Malestrom (MAEL), baculoviral inhibitor of apoptosis protein (IAP), AdintoC3, AdintoC2, and Phage T7 tail fiber proteins. The grey-colored boxes indicate ORFs that didn't show clear hits in identity in searches using BLASTP, NCBI conserved domain database and HHpred.

Fig. 6: Midguts extracted from plant-fed adults appear more green with plant content (A) compared with control midguts (B) extracted from 15% sucrose diet-fed adults with light microscopy. Autofluorescence detected using confocal microscopy in leaf-fed (C, D) and diet-fed midguts (E, F) when excited with 555 nm wavelength. Black arrowheads indicating the conical midgut portions in leaf-fed treatments contained highest plant material and had higher autofluorescence.

Fig. 7: Comparison of abundance of normalized (transcripts per million) cotton chloroplast-specific transcripts detected from RNAseq data generated from TSCL, cotton aphid (*Aphis*

gossypii), and Western flower thrips (*Frankliniella occidentalis*). Comparative higher and lower abundance of normalized transcripts is indicated with red and yellow color shading.

Fig. 8: EPG pattern from start to end of a probe by TSCL adult (A) for a duration of 97 seconds at compression of 20 (1.67 seconds/division) and nymph (B) for 702 seconds at compression 135 (11.2 seconds/division). NP denotes no probing. Vertical divisions indicate 0.71 and 1.56 V/division for adults and nymphs, respectively.

Fig. 9: Illustrated characteristics of distinct waveforms identified from the adult probe at compression 5 (0.42 seconds/division) and 0.71 V/vertical division. pd denotes potential drop.

Fig. 10: Illustrated characteristics of distinct waveforms identified from the nymph probe at compression 5 (0.42 seconds/division) and 1.56 V/vertical division.

Supplementary figure legends

Fig. S1 Phylogenetic relationship between TSCL harbored *Wolbachia* and other *Wolbachia* strains based on aligned 411 bp *FtsZ* (cell division protein) nucleotide sequences using TPM3u+F+G4 nucleotide substitution model.

Fig. S2: Wholemount control without probe for detection of *Wolbachia* using FISH (A). Midguts showing no signal for *Wolbachia* using FtsZ polyclonal antibody and Alexa Fluor™ 488 labelled anti-rabbit secondary antibody (B).

Fig. S3: Principal co-ordinate analysis (PCoA) of Bray-Curtis dissimilarities showing absence of common bacterial genera within TSCL and host plants and proves no possible involvement of TSCL transmissible bacteria as the possible causal agent of hopperburn symptoms.

Fig. S4: Hopper burn symptoms in cotton plants reared with laboratory population of TSCL (A) and mesophyll clearing on adaxial and abaxial leaf surfaces (B) attached with clip cages with TSCL adults (N=3) after 4 days of feeding.

Supplementary table legends

Table S1: Primers used in this study for PCR amplication of 16S rDNA, *Wsp* (Wolbachia surface protein), *FtsZ* (cell division protein), *Adintovirus* hexon, and polymerase B (PolB) genes.
Table S2: Abundance of bacteria genera identified by amplicon sequencing of V3-V4 (A) and full length 16S rDNA (B), and *Wolbachia* sequence variants obtained from 16s full length 16S rDNA.
Table S3: Mean read depth and abundance of *Adintovirus* contigs identified in this study (A). Annotation of DNA polymerase B (Pol B) genes against assigned Pfam families and pairwise identity RefSeq sequences of *Mayetiola barley midge adintovirus* (*alphadintovirus,* YP_010796957.1) and *Terrapene box turtle adintovirus* (*betadintovirus*, YP_010796961.1) (B).

References:

1. Shera PS, Kumar V, Jindal V. 2020. Sucking Pests of Cotton, p. 249–284. *In* Omkar (ed.), Sucking Pests of Crops. Springer Singapore, Singapore.

2. Lokesh L, Ram Singh RS. 2005. Influence of leaf vein morphology in okra genotypes (Malvaceae) on the oviposition of the leafhopper species Amrasca biguttula (Hemiptera: Cicadellidae).

3. Bindra O, Mahal M. 1981. Varietal resistance in eggplant (brinjal)(Solanum melongena) to the cotton jassid (Amrasca biguttula biguttula). Phytoparasitica 9:119–131.

4. Attia S, Joseph SV. 2025. Incidence of the Two-Spotted Cotton Leafhopper (Hemiptera: Cicadellidae) Infesting Hibiscus syriacus in Ornamentals. Agronomy 16:32.

5. Saeed R, Razaq M, Hardy IC. 2015. The importance of alternative host plants as reservoirs of the cotton leaf hopper, Amrasca devastans, and its natural enemies. J Pest Sci 88:517–531.

6. Cabrera-Asencio I, Dietrich CH, Zahniser JN. 2023. A new invasive pest in the Western Hemisphere: Amrasca biguttula (Hemiptera: Cicadellidae). Fla Entomol 106:263–266.

7. Esquivel IL, Bryant T, Malone S, Jacobson AL, Graham SH, Gimenez-Cremonez PS, Roberts P, Paula-Moreas S, Reisig D, Huseth A, Greene J, Reay-Jones FPF, Taylor S. 2025. First Report of Two-Spot Cotton Leafhopper (Amrasca biguttula Ishida) (Hemiptera: Cicadellidae) on Commercial Cotton in the Southeastern United States. Insects 16.

8. Ahmed MZ, Yadav N, Rustgi S, Saripalli G, Esquivel IL, Bryant TB, Graham S, Jacobson AL, Gireesh M, Joseph SV, Del Pozo-Valdivia A, Addesso KM, Raszick TJ, Khan R, Rodrigues JCV, Bilbo TR, Greene JK, Reay-Jones FFP. 2026. Global Phylogeography of Amrasca biguttula (Hemiptera: Cicadellidae) Across Eight Countries Reveals a Single-Haplotype Incursion Into the United States Beyond Its Putative Native Range. J Appl Entomol n/a.

9. Douglas AE. 2009. The microbial dimension in insect nutritional ecology. Funct Ecol 23:38–47.

10. Baumann P, Moran NA, Baumann L, Dworkin M. 2006. Bacteriocyte-associated endosymbionts of insects. The prokaryotes 1:403–438.

11. Cornwallis CK, van't Padje A, Ellers J, Klein M, Jackson R, Kiers ET, West SA, Henry LM. 2023. Symbioses shape feeding niches and diversification across insects. Nat Ecol Evol 7:1022–1044.

12. Takiya DM, Tran PL, Dietrich CH, Moran NA. 2006. Co-cladogenesis spanning three phyla: leafhoppers (Insecta: Hemiptera: Cicadellidae) and their dual bacterial symbionts. Mol Ecol 15:4175–4191.

13. Noda H, Watanabe K, Kawai S, Yukuhiro F, Miyoshi T, Tomizawa M, Koizumi Y, Nikoh N, Fukatsu T. 2012. Bacteriome-associated endosymbionts of the green rice leafhopper Nephotettix cincticeps (Hemiptera: Cicadellidae). Appl Entomol Zool 47:217–225.

14. Bell-Roberts L, Douglas AE, Werner GD. 2019. Match and mismatch between dietary switches and microbial partners in plant sap-feeding insects. Proc R Soc B Biol Sci 286.

15. Phauk S, Assentato L, Meas S, Terenius O. 2025. Primary and Secondary Symbionts of Cambodian Cicadellidae and the Role of Parasitisation. Environ Microbiol Rep 17:e70196.

16. Cooper WR, Walker III WB, Angelella GM, Swisher Grimm KD, Foutz JJ, Harper SJ, Nottingham LB, Northfield TD, Wohleb CH, Strausbaugh CA. 2023. Bacterial endosymbionts identified from leafhopper (Hemiptera: Cicadellidae) vectors of phytoplasmas. Environ Entomol 52:243–253.

17. Kobiałka M, Świerczewski D, Walczak M, Urbańczyk W. 2025. Extremely distinct microbial communities in closely related leafhopper subfamilies: *Typhlocybinae* and Eurymelinae (Cicadellidae, Hemiptera). Msystems 10:e00603-25.

18. Kobiałka M, Michalik A, Szwedo J, Szklarzewicz T. 2018. Diversity of symbiotic microbiota in Deltocephalinae leafhoppers (Insecta, Hemiptera, Cicadellidae). Arthropod Struct Dev 47:268–278.

19. Himler AG, Adachi-Hagimori T, Bergen JE, Kozuch A, Kelly SE, Tabashnik BE, Chiel E, Duckworth VE, Dennehy TJ, Zchori-Fein E, Hunter MS. 2011. Rapid spread of a bacterial symbiont in an invasive whitefly is driven by fitness benefits and female bias. Science 332:254–6.

20. Montllor CB, Maxmen A, Purcell AH. 2002. Facultative bacterial endosymbionts benefit pea aphids Acyrthosiphon pisum under heat stress. Ecol Entomol 27:189–195.

21. Oliver KM, Russell JA, Moran NA, Hunter MS. 2003. Facultative bacterial symbionts in aphids confer resistance to parasitic wasps. Proc Natl Acad Sci 100:1803–1807.

22. Hendry TA, Hunter MS, Baltrus DA. 2014. The Facultative Symbiont Rickettsia Protects an Invasive Whitefly against Entomopathogenic Pseudomonas syringae Strains. Appl Environ Microbiol 80:7161–7168.

23. Hansen AK, Jeong G, Paine TD, Stouthamer R. 2007. Frequency of secondary symbiont infection in an invasive psyllid relates to parasitism pressure on a geographic scale in California. Appl Environ Microbiol 73:7531–7535.

24. Oliver KM, Moran NA, Hunter MS. 2006. Costs and benefits of a superinfection of facultative symbionts in aphids. Proc R Soc B Biol Sci 273:1273–1280.

25. Ghosh S, Bouvaine S, Richardson SC, Ghanim M, Maruthi M. 2018. Fitness costs associated with infections of secondary endosymbionts in the cassava whitefly species Bemisia tabaci. J Pest Sci 91:17–28.

26. Li S-J, Ahmed MZ, Lv N, Shi P-Q, Wang X-M, Huang J-L, Qiu B-L. 2017. Plant–mediated horizontal transmission of Wolbachia between whiteflies. ISME J 11:1019–1028.

27. Gonella E, Pajoro M, Marzorati M, Crotti E, Mandrioli M, Pontini M, Bulgari D, Negri I, Sacchi L, Chouaia B. 2015. Plant-mediated interspecific horizontal transmission of an intracellular symbiont in insects. Sci Rep 5:15811.

28. Caspi-Fluger A, Inbar M, Mozes-Daube N, Katzir N, Portnoy V, Belausov E, Hunter MS, Zchori-Fein E. 2011. Horizontal transmission of the insect symbiont Rickettsia is plant-mediated. Proc R Soc B Biol Sci rspb20112095.

29. Frago E, Dicke M, Godfray HCJ. 2012. Insect symbionts as hidden players in insect–plant interactions. Trends Ecol Evol 27:705–711.

30. Douglas AE. 2015. Multiorganismal insects: diversity and function of resident microorganisms. Annu Rev Entomol 60:17–34.

31. Lv C, Xia Q, Yan S. 2026. Symbiont-mediated mechanisms of insecticide resistance in insects. J Insect Sci 26:ieag042.

32. Cao Y, Dietrich CH, Kits JH, Dmitriev DA, Richter R, Eyres J, Dettman JR, Xu Y, Huang M. 2023. Phylogenomics of microleafhoppers (Hemiptera: Cicadellidae: *Typhlocybinae*): morphological evolution, divergence times, and biogeography. Insect Syst Divers 7:1.

33. Hunter WB, Backus EA. 1989. Mesophyll-feeding by the potato leafhopper, Empoasca fabae (Homoptera: Cicadellidae): results from electronic monitoring and thin-layer chromatography. Environ Entomol 18:465–472.

34. Tonkyn DW, Whitcomb RF. 1987. Feeding strategies and the guild concept among vascular feeding insects and microorganisms, p. 179–199. *In* Current Topics in Vector Research: Volume 4. Springer.

35. Aguin-Pombo D, Rodrigues MC, Voetdijk B, Breeuwer JA. 2021. Parthenogenesis and sex-ratio distorting bacteria in Empoasca (Hemiptera: Cicadellidae) Leafhoppers. Ann Entomol Soc Am 114:738–749.

36. DeLay BD. 2013. Symbionts associated with the salivary glands of the potato leafhopper, Empoasca fabae, and their function when feeding on leguminous hosts.

37. Caporaso JG, Kuczynski J, Stombaugh J, Bittinger K, Bushman FD, Costello EK, Fierer N, Peña AG, Goodrich JK, Gordon JI. 2010. QIIME allows analysis of high-throughput community sequencing data. Nat Methods 7:335–336.

38. RCoreTeam. 2025. R: A Language and Environment for Statistical Computing4.4.3. R Foundation for Statistical Computing, Vienna, Austria.

39. Ghosh S, Sela N, Kontsedalov S, Lebedev G, Haines LR, Ghanim M. 2020. An intranuclear sodalis-like symbiont and spiroplasma coinfect the carrot psyllid, bactericera trigonica (Hemiptera, psylloidea). Microorganisms 8.

40. Ghosh S, Bouvaine S, Maruthi MN. 2015. Prevalence and genetic diversity of endosymbiotic bacteria infecting cassava whiteflies in Africa. BMC Microbiol 15:93.

41. Wong TK, Ly-Trong N, Ren H, Demotte P, Baños H, Roger AJ, Susko E, Bielow C, De Maio N, Goldman N. 2026. IQ-TREE 3: phylogenomic inference software using complex evolutionary models. Mol Biol Evol 43:msag117.

42. Letunic I, Bork P. 2024. Interactive Tree of Life (iTOL) v6: recent updates to the phylogenetic tree display and annotation tool. Nucleic Acids Res 52:W78–W82.

43. Kliot A, Kontsedalov S, Lebedev G, Brumin M, Cathrin PB, Marubayashi JM, Skaljac M, Belausov E, Czosnek H, Ghanim M. 2014. Fluorescence in situ hybridizations (FISH) for the localization of viruses and endosymbiotic bacteria in plant and insect tissues. J Vis Exp JoVE 84:e51030.

44. Ghanim M, Achor D, Ghosh S, Kontsedalov S, Lebedev G, Levy A. 2017. 'Candidatus Liberibacter asiaticus' Accumulates inside Endoplasmic Reticulum Associated Vacuoles in the Gut Cells of Diaphorina citri. Sci Rep 7:16945.

45. Andrews S. 2010. FastQC: a quality control tool for high throughput sequence datahttp. Bioinformaticsbabraham Ac Ukprojectsfastqc.

46. Ewels P, Magnusson M, Lundin S, Käller M. 2016. MultiQC: summarize analysis results for multiple tools and samples in a single report. Bioinformatics 32:3047–3048.

47. Bushmanova E, Antipov D, Lapidus A, Prjibelski AD. 2019. rnaSPAdes: a de novo transcriptome assembler and its application to RNA-Seq data. GigaScience 8:giz100.

48. Buchfink B, Reuter K, Drost H-G. 2021. Sensitive protein alignments at tree-of-life scale using DIAMOND. Nat Methods 18:366–368.

49. Pandey S, Catto M, Roberts P, Bag S, Jacobson AL, Srinivasan R. 2024. Aphid gene expression following polerovirus acquisition is host species dependent. Front Plant Sci Volume 15-2024.

50. Dobin A, Davis CA, Schlesinger F, Drenkow J, Zaleski C, Jha S, Batut P, Chaisson M, Gingeras TR. 2013. STAR: ultrafast universal RNA-seq aligner. Bioinformatics 29:15–21.

51. Pertea M, Kim D, Pertea GM, Leek JT, Salzberg SL. 2016. Transcript-level expression analysis of RNA-seq experiments with HISAT, StringTie and Ballgown. Nat Protoc 11:1650–1667.

52. Walker GP, Fereres A, Tjallingii W. 2024. Guidelines for conducting, analyzing, and interpreting electrical penetration graph (EPG) experiments on herbivorous piercing–sucking insects. Entomol Exp Appl 172:564–580.

53. DeLay B, Mamidala P, Wijeratne A, Wijeratne S, Mittapalli O, Wang J, Lamp W. 2012. Transcriptome analysis of the salivary glands of potato leafhopper, Empoasca fabae. J Insect Physiol 58:1626–1634.

54. Rasool B, Zafar S, Younis T, Zafar S, Parvaiz A, Akhtar Y, Javed Z, Ahmad W. 2026. Exploration of Wolbachia strains in Amrasca biguttula Ishida (Hemiptera: Cicadellidae) and its egg parasitoid Trichogramma chilonis (Hymenoptera: Trichogrammatidae). BMC Microbiol.

55. Henke C, Nickel H, Scheu S, Schaeffer I. 2013. Evidence for Wolbachia in leafhoppers of the genus Eupteryx with intersexual morphotypes. Bull Insectology 66:109–118.

56. Ijichi N, Kondo N, Matsumoto R, Shimada M, Ishikawa H, Fukatsu T. 2002. Internal spatiotemporal population dynamics of infection with three Wolbachia strains in the adzuki bean beetle, Callosobruchus chinensis (Coleoptera: Bruchidae). Appl Environ Microbiol 68:4074–4080.

57. Roehrdanz RL, Sears Wichmann SG. 2013. Wolbachia wsp gene clones detect the distribution of Wolbachia variants and wsp hypervariable regions among individuals of a multistrain infected population of Diabrotica barberi (Coleoptera: Chrysomelidae). Ann Entomol Soc Am 106:329–338.

58. Martinez J, Ross PA, Gu X, Ant TH, Murdochy SM, Tong L, da Silva Filipe A, Hoffmann AA, Sinkins SP. 2022. Genomic and phenotypic comparisons reveal distinct variants of Wolbachia Strain w AlbB. Appl Environ Microbiol 88:e01412-22.

59. Werren JH, Baldo L, Clark ME. 2008. Wolbachia: master manipulators of invertebrate biology. Nat Rev Microbiol 6:741–51.

60. Negri I, Pellecchia M, Mazzoglio PJ, Patetta A, Alma A. 2006. Feminizing Wolbachia in Zyginidia pullula (Insecta, Hemiptera), a leafhopper with an XX/X0 sex-determination system. Proc R Soc B Biol Sci 273:2409–2416.

61. Noda H, Koizumi Y, Zhang Q, Deng K. 2001. Infection density of Wolbachia and incompatibility level in two planthopper species, Laodelphax striatellus and Sogatella furcifera. Insect Biochem Mol Biol 31:727–737.

62. Ju J-F, Bing X-L, Zhao D-S, Guo Y, Xi Z, Hoffmann AA, Zhang K-J, Huang H-J, Gong J-T, Zhang X. 2020. Wolbachia supplement biotin and riboflavin to enhance reproduction in planthoppers. ISME J 14:676–687.

63. Pan X, Zhou G, Wu J, Bian G, Lu P, Raikhel AS, Xi Z. 2012. Wolbachia induces reactive oxygen species (ROS)-dependent activation of the Toll pathway to control dengue virus in the mosquito Aedes aegypti. Proc Natl Acad Sci 109:E23–E31.

64. Audsley MD, Seleznev A, Joubert DA, Woolfit M, O'Neill SL, McGraw EA. 2018. Wolbachia infection alters the relative abundance of resident bacteria in adult Aedes aegypti mosquitoes, but not larvae. Mol Ecol 27:297–309.

65. Thekke-Veetil T, Lagos-Kutz D, Domier LL, McCoppin NK, Hartman GL, Clough SJ. 2024. Exploring virus diversity in the potato leafhopper (Empoasca fabae), an economically important agricultural pest. Viruses 16:1305.

66. Neuman BW, Smart A, Gilmer O, Smyth RP, Vaas J, Böker N, Samborskiy DV, Bartenschlager R, Seitz S, Gorbalenya AE. 2025. Giant RNA genomes: Roles of host, translation elongation, genome architecture, and proteome in nidoviruses. Proc Natl Acad Sci 122:e2413675122.

67. Lahey Z, Jones T-KL, Simmons AM, Andreason SA. 2026. In silico detection and characterization of novel Picornavirales mined from publicly available insect RNA-seq data sets. Microbiol Spectr 14:e01701-25.

68. Krupovic M, Koonin EV. 2015. Polintons: a hotbed of eukaryotic virus, transposon and plasmid evolution. Nat Rev Microbiol 13:105–115.

69. Starrett GJ, Tisza MJ, Welch NL, Belford AK, Peretti A, Pastrana DV, Buck CB. 2021. Adintoviruses: a proposed animal-tropic family of midsize eukaryotic linear dsDNA (MELD) viruses. Virus Evol 7:veaa055.

70. Fischer MG, Hackl T. 2016. Host genome integration and giant virus-induced reactivation of the virophage mavirus. Nature 540:288–291.

71. Parker BJ, Rozo-Lopez P. 2025. Heritable Viruses as Hidden Drivers of Insect Phenotypes and Evolution. Annu Rev Entomol 71.

72. Jacobs S. 2001. Review of leaf anatomy and ultrastructure in the Chenopodiaceae (Caryophyllales). J Torrey Bot Soc 236–253.

73. Barton KA, Schattat MH, Jakob T, Hause G, Wilhelm C, Mckenna JF, Máthé C, Runions J, Van Damme D, Mathur J. 2016. Epidermal pavement cells of Arabidopsis have chloroplasts. Plant Physiol 171:723–726.

74. Jin S, Chen ZM, Backus EA, Sun XL, Xiao B. 2012. Characterization of EPG waveforms for the tea green leafhopper, Empoasca vitis Göthe (Hemiptera: Cicadellidae), on tea plants and their correlation with stylet activities. J Insect Physiol 58:1235–1244.

75. Backus EA, Serrano MS, Ranger CM. 2005. Mechanisms of hopperburn: an overview of insect taxonomy, behavior, and physiology. Annu Rev Entomol 50:125–151.

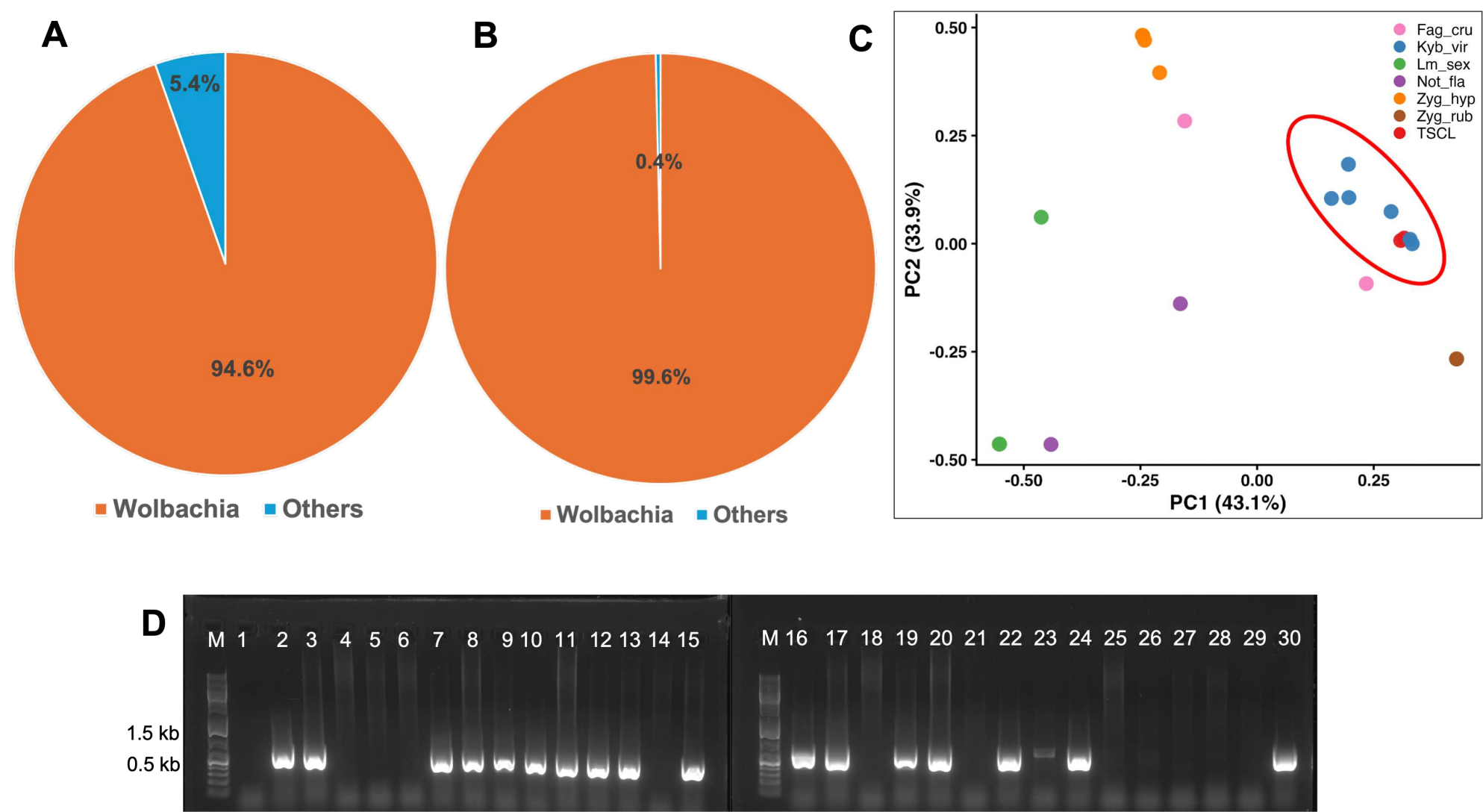
76. Tariq K, Noor M, Backus EA, Hussain A, Ali A, Peng W, Zhang H. 2017. The toxicity of flonicamid to cotton leafhopper, Amrasca biguttula (Ishida), is by disruption of ingestion: an electropenetrography study. Pest Manag Sci 73:1661–1669.

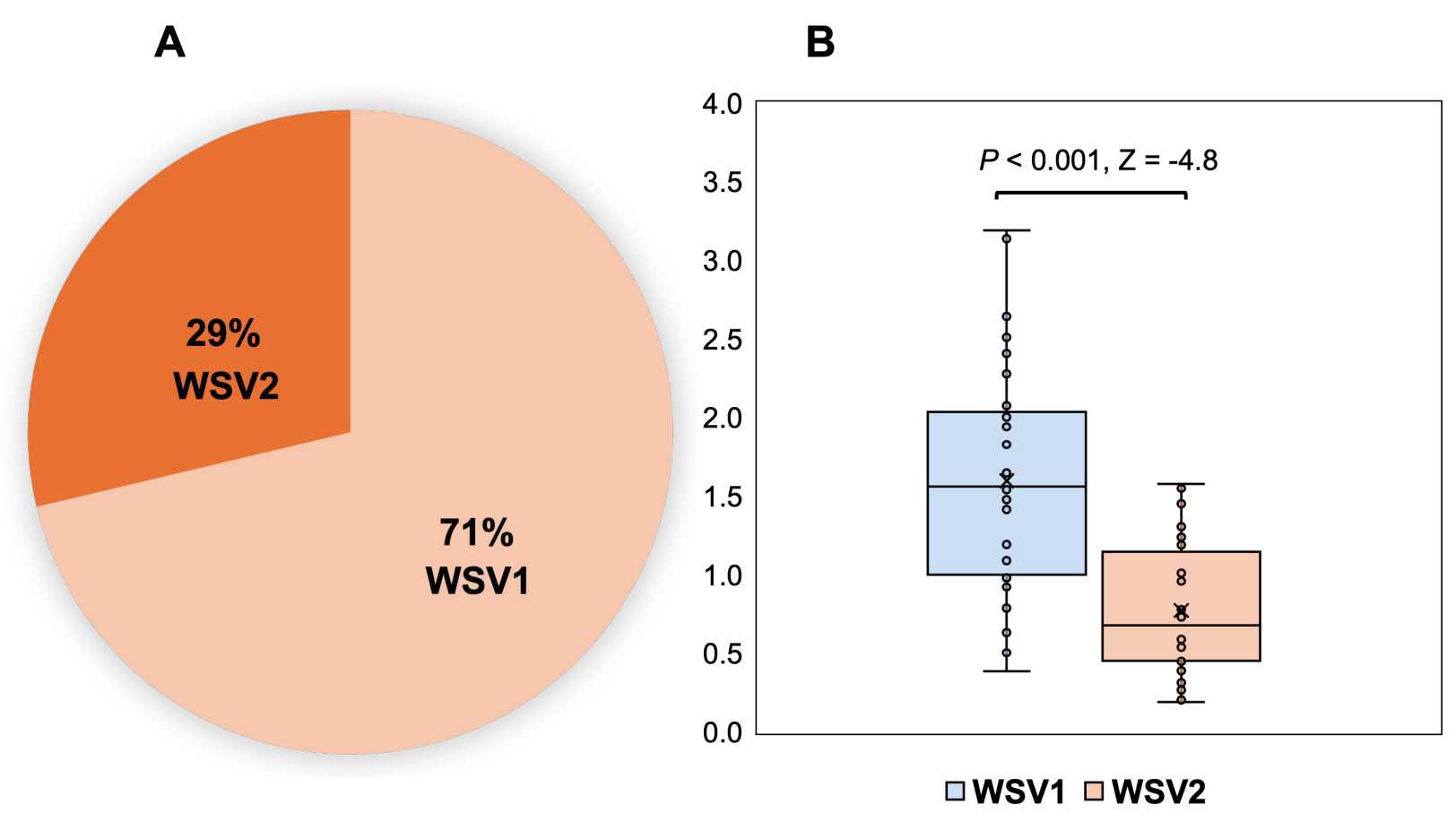
77. Biswas C, Dey P, Bera A, Kumar M, Satpathy S. 2014. First report of a 16SrV-C phytoplasma causing little leaf and bunchy top of tossa jute (Corchorus olitorius) in India. Plant Dis 98:565–565.

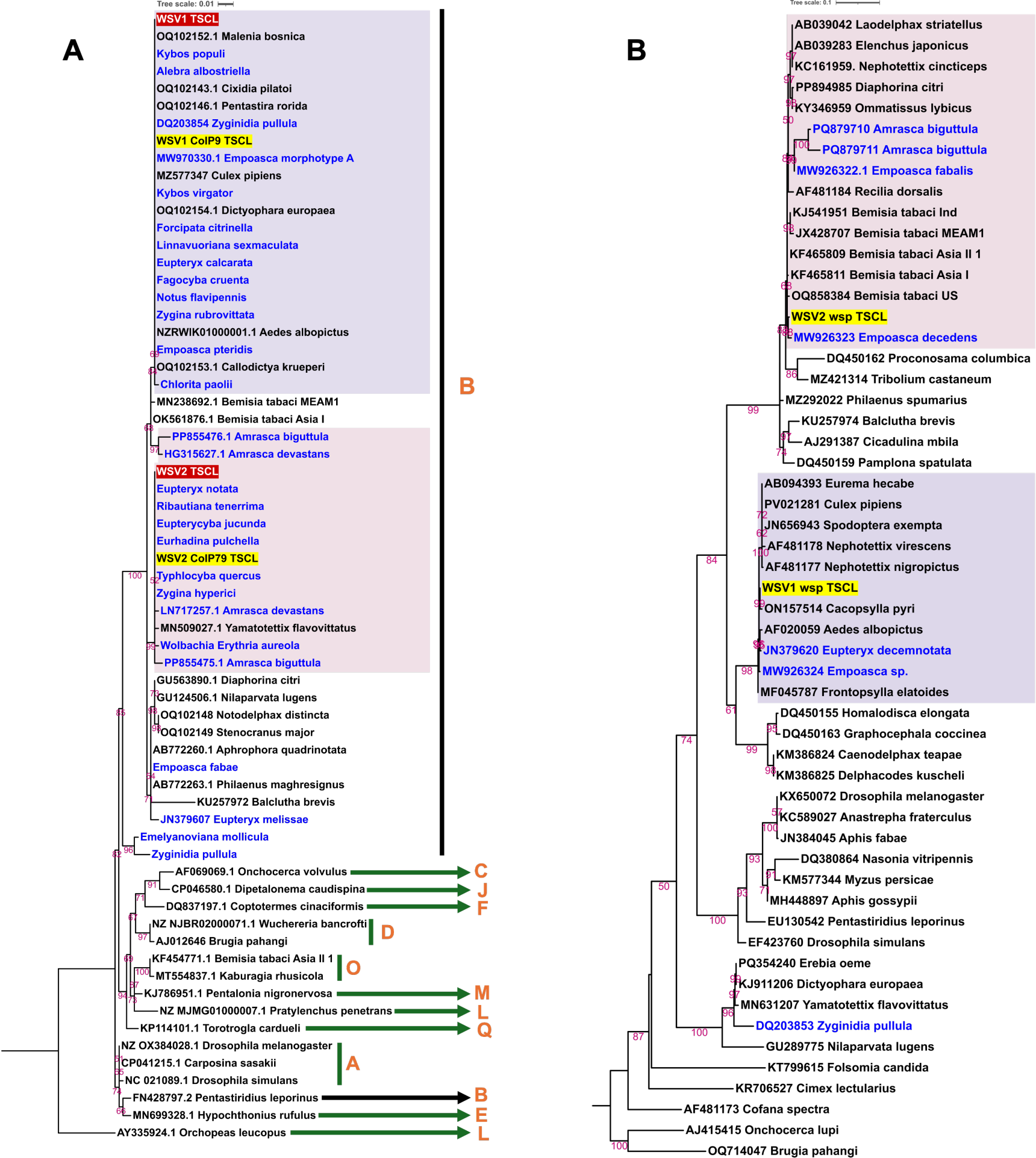
78. Gopala, Rao GP. 2018. Molecular characterization of phytoplasma associated with four important ornamental plant species in India and identification of natural potential spread sources. 3 Biotech 8:116.

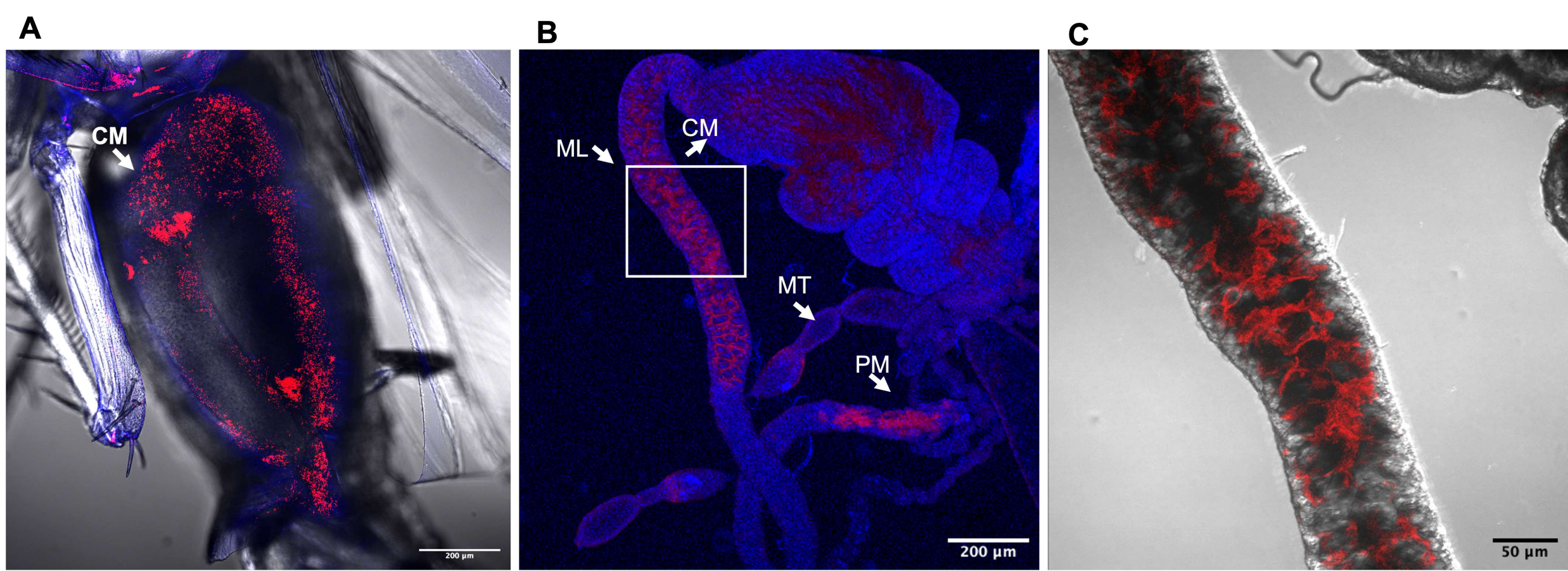
79. Reddy MG, Baranwal VK, Sagar D, Rao GP. 2021. Molecular characterization of chickpea chlorotic dwarf virus and peanut witches' broom phytoplasma associated

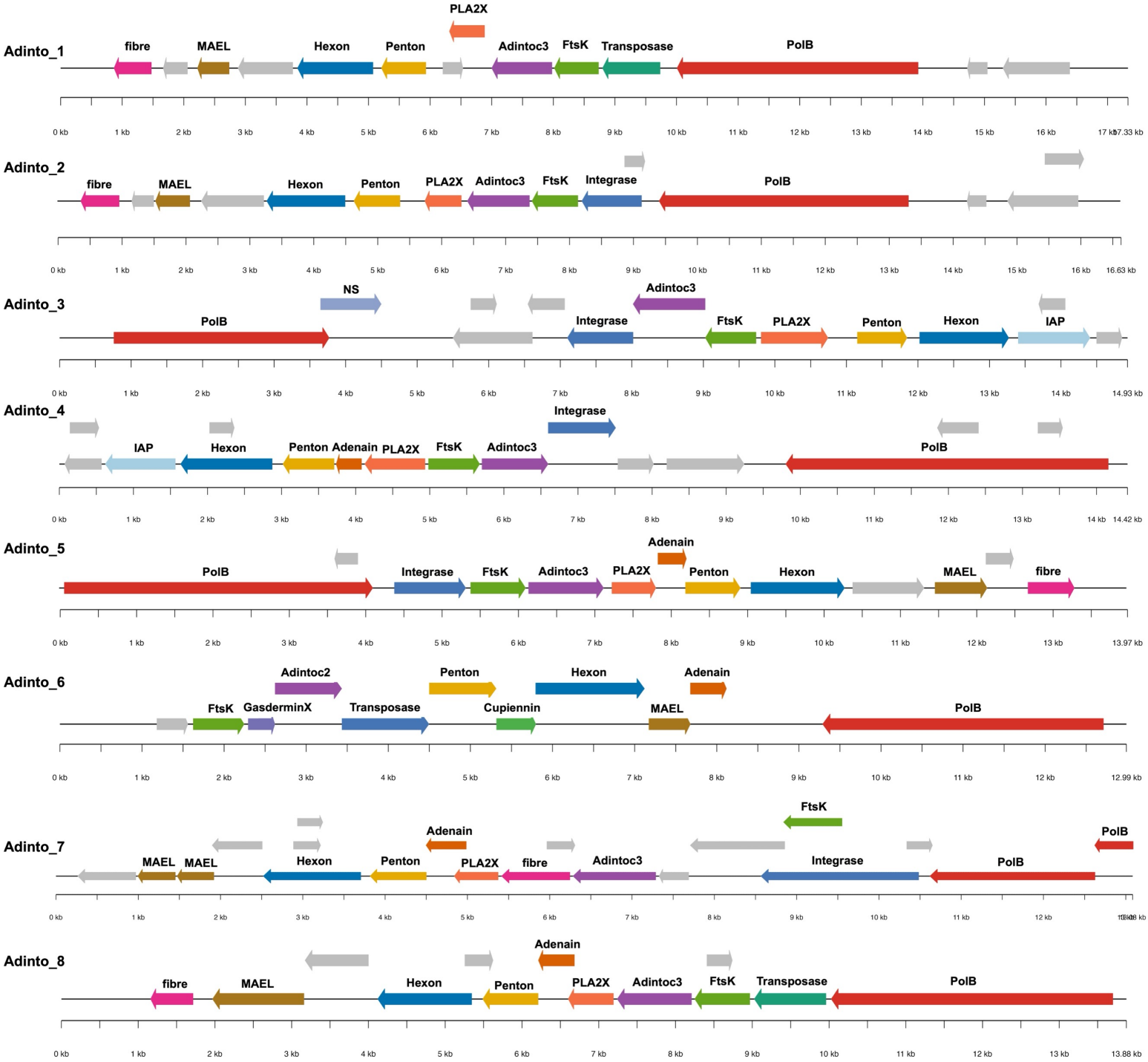
with chickpea stunt disease and identification of new host crops and leafhopper vectors in India. 3 Biotech 11:112.

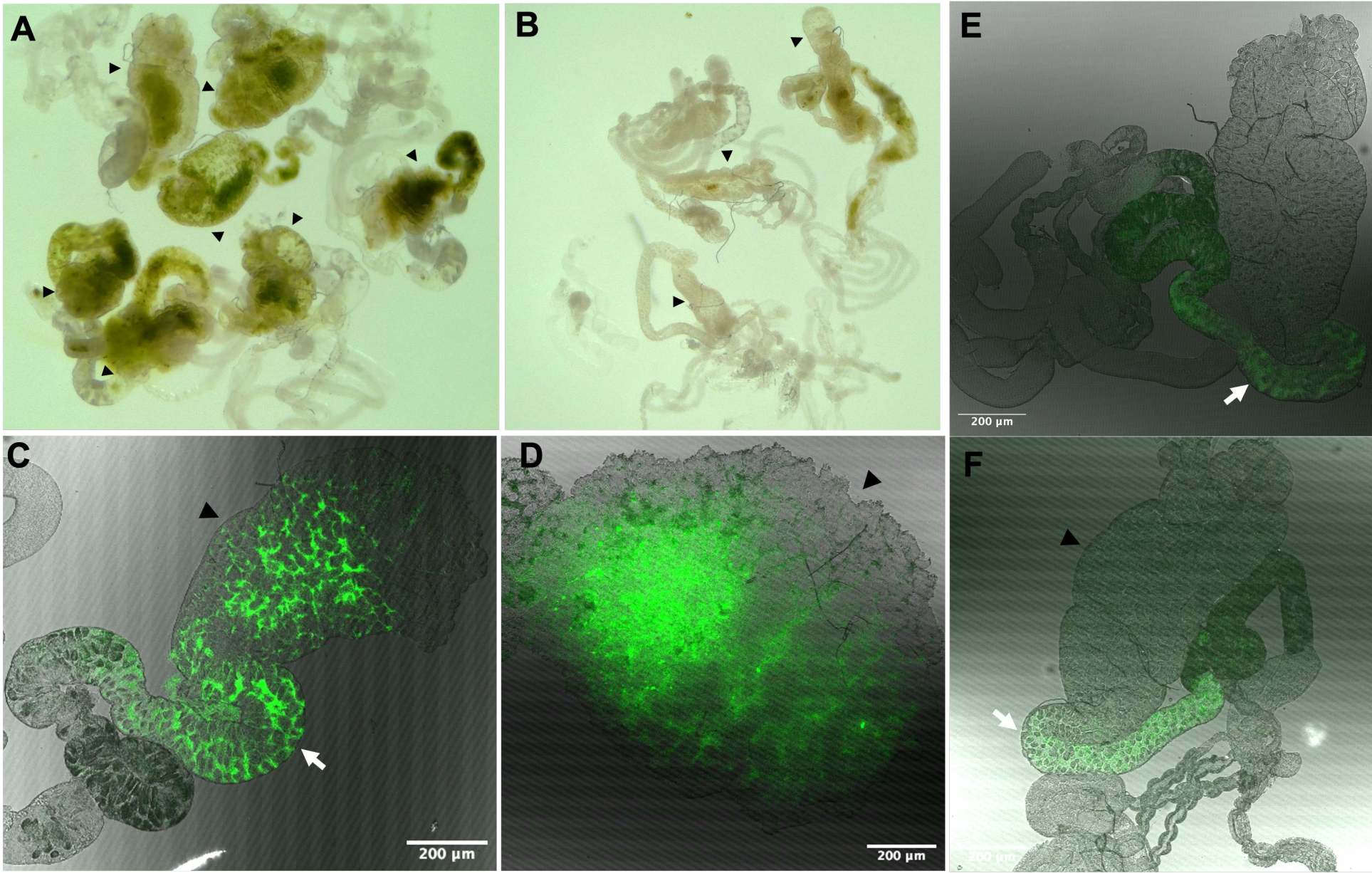

A
5.4%
94.6%
Wolbachia
Others
B
0.4%
99.6%
Wolbachia
Others
C
Fag_cru
Kyb_vir
Lm_sex
Not_fla
Zyg_hyp
Zyg_rub
TSCL
PC2 (33.9%)
PC1 (43.1%)
0.50
0.25
0.00
-0.25
-0.50
D
M 1 2 3 4 5 6 7 8 9 10 11 12 13 14 15
M 16 17 18 19 20 21 22 23 24 25 26 27 28 29 30
1.5 kb
0.5 kb


A
29%
WSV2
71%
WSV1
B
4.0
3.5
3.0
2.5
2.0
1.5
1.0
0.5
0.0
P < 0.001, Z = -4.8
WSV1
WSV2

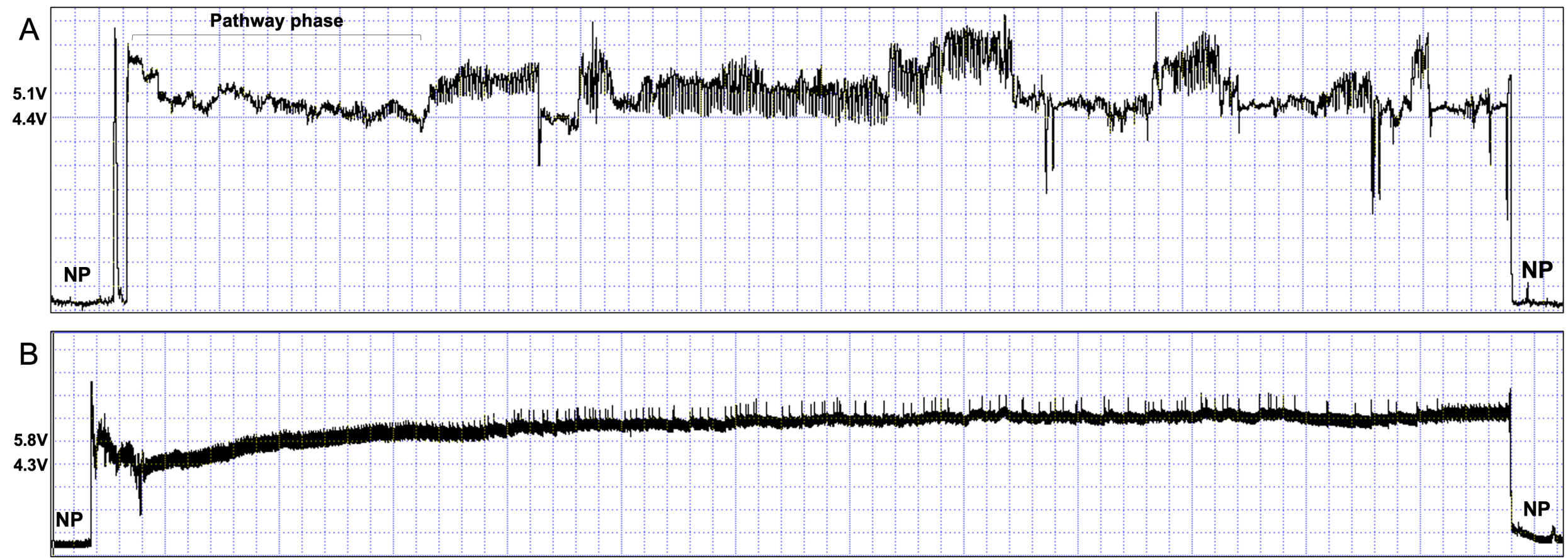

A
Tree scale: 0.01
WSV1 TSCL
OQ102152.1 Malenia bosnica
Kybos populi
Alebra albostriella
OQ102143.1 Cixidia pilatoi
OQ102146.1 Pentastira rorida
DQ203854 Zyginidia pullula
WSV1 ColP9 TSCL
MW970330.1 Empoasca morphotype A
MZ577347 Culex pipiens
Kybos virgator
OQ102154.1 Dictyophara europaea
Forcipata citrinella
Linnavuoriana sexmaculata
Eupteryx calcarata
Fagocyba cruenta
Notus flavipennis
Zygina rubrovittata
NZRWIK01000001.1 Aedes albopictus
Empoasca pteridis
OQ102153.1 Callodictya krueperi
Chlorita paolii
MN238692.1 Bemisia tabaci MEAM1
OK561876.1 Bemisia tabaci Asia I
PP855476.1 Amrasca biguttula
HG315627.1 Amrasca devastans
WSV2 TSCL
Eupteryx notata
Ribautiana tenerrima
Eupterycyba jucunda
Eurhadina pulchella
WSV2 ColP79 TSCL
Typhlocyba quercus
Zygina hyperici
LN717257.1 Amrasca devastans
MN509027.1 Yamatotettix flavovittatus
Wolbachia Erythria aureola
PP855475.1 Amrasca biguttula
GU563890.1 Diaphorina citri
GU124506.1 Nilaparvata lugens
OQ102148 Notodelphax distincta
OQ102149 Stenocranus major
AB772260.1 Aphrophora quadrinotata
Empoasca fabae
AB772263.1 Philaenus maghresignus
KU257972 Balclutha brevis
JN379607 Eupteryx melissae
Emelyanoviana mollicula
Zyginidia pullula
AF069069.1 Onchocerca volvulus
CP046580.1 Dipetalonema caudispina
DQ837197.1 Coptotermes cinaciformis
NZ NJBR02000071.1 Wuchereria bancrofti
AJ012646 Brugia pahangi
KF454771.1 Bemisia tabaci Asia II 1
MT554837.1 Kaburagia rhusicola
KJ786951.1 Pentalonia nigronervosa
NZ MJMG01000007.1 Pratylenchus penetrans
KP114101.1 Torotrogla cardueli
NZ OX384028.1 Drosophila melanogaster
CP041215.1 Carposina sasakii
NC 021089.1 Drosophila simulans
FN428797.2 Pentastiridius leporinus
MN699328.1 Hypochthonius rufulus
AY335924.1 Orchopeas leucopus
B
C
J
F
D
O
M
L
Q
A
B
E
L
B
Tree scale: 0.1
AB039042 Laodelphax striatellus
AB039283 Elenchus japonicus
KC161959. Nephotettix cincticeps
PP894985 Diaphorina citri
KY346959 Ommatissus lybicus
PQ879710 Amrasca biguttula
PQ879711 Amrasca biguttula
MW926322.1 Empoasca fabalis
AF481184 Recilia dorsalis
KJ541951 Bemisia tabaci Ind
JX428707 Bemisia tabaci MEAM1
KF465809 Bemisia tabaci Asia II 1
KF465811 Bemisia tabaci Asia I
OQ858384 Bemisia tabaci US
WSV2 wsp TSCL
MW926323 Empoasca decedens
DQ450162 Proconosama columbica
MZ421314 Tribolium castaneum
MZ292022 Philaenus spumarius
KU257974 Balclutha brevis
AJ291387 Cicadulina mbila
DQ450159 Pamplona spatulata
AB094393 Eurema hecabe
PV021281 Culex pipiens
JN656943 Spodoptera exempta
AF481178 Nephotettix virescens
AF481177 Nephotettix nigropictus
WSV1 wsp TSCL
ON157514 Cacopsylla pyri
AF020059 Aedes albopictus
JN379620 Eupteryx decemnotata
MW926324 Empoasca sp.
MF045787 Frontopsylla elatoides
DQ450155 Homalodisca elongata
DQ450163 Graphocephala coccinea
KM386824 Caenodelphax teapae
KM386825 Delphacodes kuscheli
KX650072 Drosophila melanogaster
KC589027 Anastrepha fraterculus
JN384045 Aphis fabae
DQ380864 Nasonia vitripennis
KM577344 Myzus persicae
MH448897 Aphis gossypii
EU130542 Pentastiridius leporinus
EF423760 Drosophila simulans
PQ354240 Erebia oeme
KJ911206 Dictyophara europaea
MN631207 Yamatotettix flavovittatus
DQ203853 Zyginidia pullula
GU289775 Nilaparvata lugens
KT799615 Folsomia candida
KR706527 Cimex lectularius
AF481173 Cofana spectra
AJ415415 Onchocerca lupi
OQ714047 Brugia pahangi

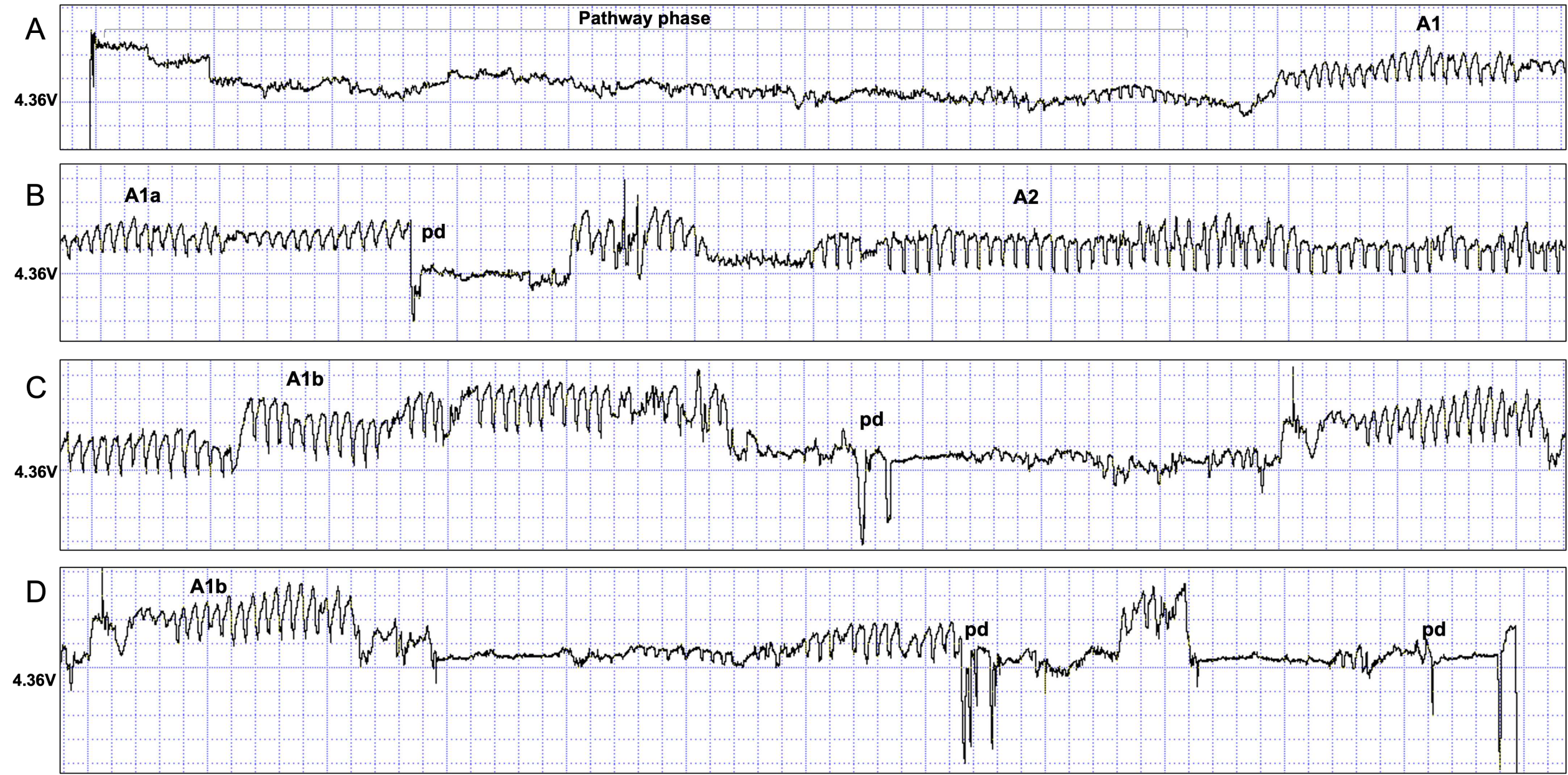

A
CM
200 µm
B
ML
CM
MT
PM
200 µm
C
50 µm

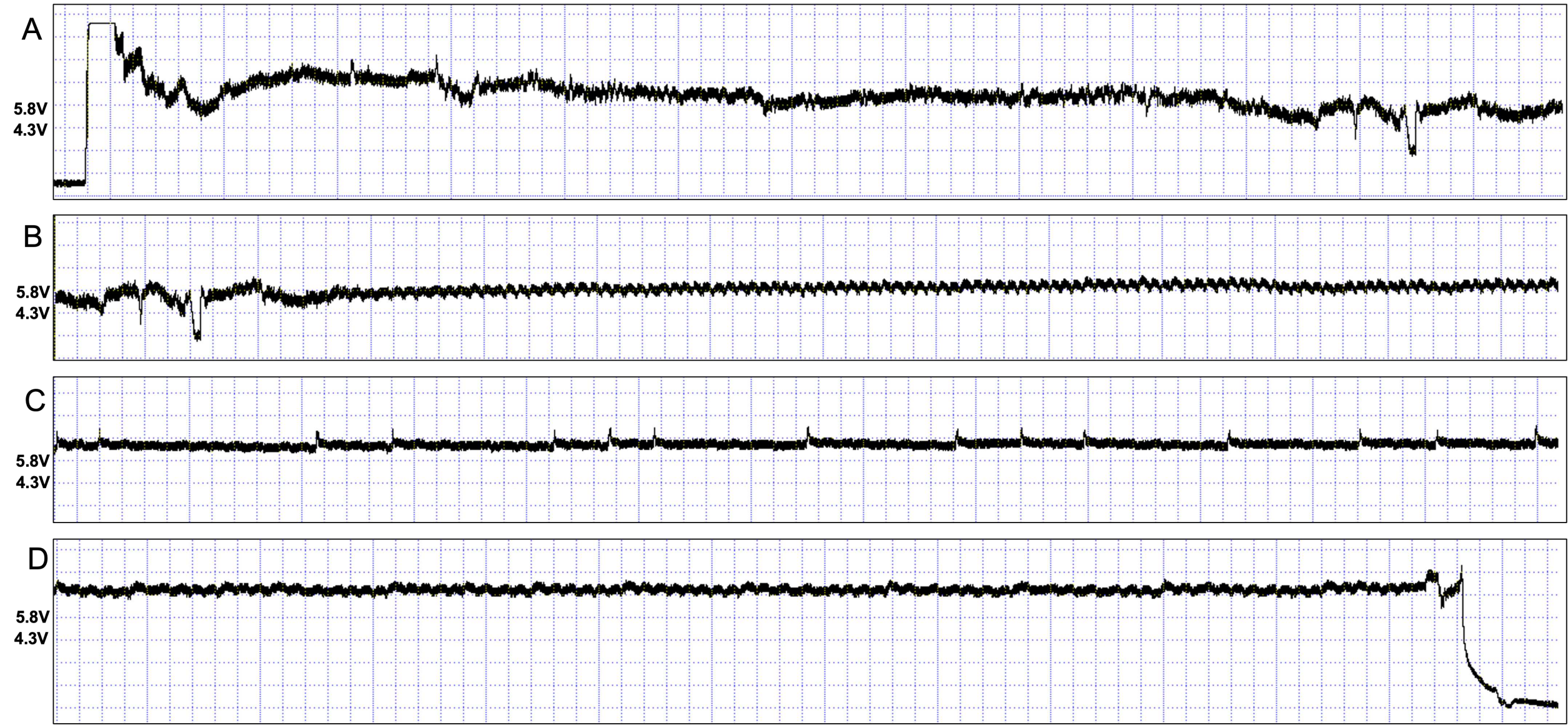

Adinto_1
PLA2X
fibre
MAEL
Hexon
Penton
Adintoc3
FtsK
Transposase
PolB
0 kb 1 kb 2 kb 3 kb 4 kb 5 kb 6 kb 7 kb 8 kb 9 kb 10 kb 11 kb 12 kb 13 kb 14 kb 15 kb 16 kb 17 kb 17.33 kb
Adinto_2
fibre
MAEL
Hexon
Penton
PLA2X
Adintoc3
FtsK
Integrase
PolB
0 kb 1 kb 2 kb 3 kb 4 kb 5 kb 6 kb 7 kb 8 kb 9 kb 10 kb 11 kb 12 kb 13 kb 14 kb 15 kb 16 kb 16.63 kb
Adinto_3
NS
Adintoc3
PolB
Integrase
FtsK
PLA2X
Penton
Hexon
IAP
0 kb 1 kb 2 kb 3 kb 4 kb 5 kb 6 kb 7 kb 8 kb 9 kb 10 kb 11 kb 12 kb 13 kb 14 kb 14.93 kb
Adinto_4
Integrase
IAP
Hexon
Penton
Adenain
PLA2X
FtsK
Adintoc3
PolB
0 kb 1 kb 2 kb 3 kb 4 kb 5 kb 6 kb 7 kb 8 kb 9 kb 10 kb 11 kb 12 kb 13 kb 14 kb 14.42 kb
Adinto_5
Adenain
PolB
Integrase
FtsK
Adintoc3
PLA2X
Penton
Hexon
MAEL
fibre
0 kb 1 kb 2 kb 3 kb 4 kb 5 kb 6 kb 7 kb 8 kb 9 kb 10 kb 11 kb 12 kb 13 kb 13.97 kb
Adinto_6
Adintoc2
Penton
Hexon
Adenain
FtsK
GasderminX
Transposase
Cupiennin
MAEL
PolB
0 kb 1 kb 2 kb 3 kb 4 kb 5 kb 6 kb 7 kb 8 kb 9 kb 10 kb 11 kb 12 kb 12.99 kb
Adinto_7
FtsK
Adenain
PolB
MAEL
MAEL
Hexon
Penton
PLA2X
fibre
Adintoc3
Integrase
PolB
0 kb 1 kb 2 kb 3 kb 4 kb 5 kb 6 kb 7 kb 8 kb 9 kb 10 kb 11 kb 12 kb
Adinto_8
Adenain
fibre
MAEL
Hexon
Penton
PLA2X
Adintoc3
FtsK
Transposase
PolB
0 kb 1 kb 2 kb 3 kb 4 kb 5 kb 6 kb 7 kb 8 kb 9 kb 10 kb 11 kb 12 kb 13 kb 13.88 kb


A
B
E
200 µm
C
200 µm
D
200 µm
F

Gene name	TSLH	*A. gossypii*	*F. occidentalis*	Annotation
GohiCr003	75.7	0.0	0.0	4.5S rRNA
GohiCr006	75.9	0.0	0.0	4.5S rRNA
GohiCr004	0.0	0.0	67.0	5S rRNA
GohiCr005	0.0	0.0	67.0	5S rRNA
GohiCr001	2163.5	136.0	3231.8	16S rRNA
GohiCr008	2168.8	39.6	3281.4	16S rRNA
GohiCr007	6625.7	6.9	3231.8	23S rRNA
GohiCr002	6624.3	2.5	9026.5	23S rRNA
rps2	50.4	0.0	0.0	30S Ribosomal protein
rps4	28.9	0.0	0.0	30S Ribosomal protein
rps7	40.0	0.0	5.0	30S Ribosomal protein
rps8	22.6	0.0	0.0	30S Ribosomal protein
rps11	304.3	0.0	0.0	30S Ribosomal protein
rps14	58.4	0.0	0.0	30S Ribosomal protein
rps15	435.9	0.0	0.0	30S Ribosomal protein
rps19	56.9	0.0	0.0	30S Ribosomal protein
rpl36	100.4	0.0	0.0	50S Ribosomal protein
atpA	298.5	0.0	0.0	ATP synthase CF1 complex
atpB	54.8	0.0	0.0	ATP synthase CF1 complex
atpE	219.4	0.0	0.0	ATP synthase CF1 complex
atpH	93.7	0.0	0.0	ATP synthase CF0 complex
atpI	0.0	0.0	37.6	ATP synthase CF0 complex
matK	6.8	0.0	0.0	Chloroplast RNA splicing
cemA	111.1	0.0	48.5	Chloroplast membrane
ycf1	2.7	0.0	0.0	Chloroplast membrane
petA	277.7	0.0	35.2	Cytochrome b6/f complex
petD	218.2	0.0	57.6	Cytochrome b6/f complex
ndhB	0.0	0.0	5.4	NADH dehydrogenase complex
ndhC	75.1	0.0	0.0	NADH dehydrogenase complex
ndhD	0.0	0.0	10.7	NADH dehydrogenase complex
ndhG	12.3	0.0	0.0	NADH dehydrogenase complex
ndhI	204.9	0.0	0.0	NADH dehydrogenase complex
ndhJ	26.0	0.0	0.0	NADH dehydrogenase complex
ndhK	153.4	0.0	0.0	NADH dehydrogenase complex
psaA	220.0	0.0	0.0	Photosystem I
psaB	181.5	0.0	80.8	Photosystem I
psaC	209.6	0.0	0.0	Photosystem I
ycf4	93.7	0.0	0.0	Photosystem I assembly
psbA	2044.6	0.0	2644.5	Photosystem II
psbB	108.5	0.0	27.0	Photosystem II
psbC	186.5	0.0	118.8	Photosystem II
psbD	109.6	0.0	57.6	Photosystem II
psbE	108.5	0.0	32.9	Photosystem II
psbF	0.0	0.0	156.3	Photosystem II
psbH	113.0	0.0	0.0	Photosystem II
psbL	0.0	0.0	38.7	Photosystem II
psbT	394.5	0.0	0.0	Photosystem II
rbcL	506.1	0.0	66.2	Rubisco
rpoB	10.7	0.0	0.0	RNA polymerase complex
rpoC1	778.9	0.0	0.0	RNA polymerase complex
rpoC2	12.1	0.0	0.0	RNA polymerase complex
trnA	135.6	0.0	0.0	tRNA-Alanine
trnL	185.1	0.0	0.0	tRNA-Leucine
trnP	233.7	0.0	0.0	tRNA-Proline


A
Pathway phase
5.1V
4.4V
NP
NP
B
5.8V
4.3V
NP
NP


A
Pathway phase
A1
4.36V
B
A1a
pd
A2
4.36V
C
A1b
pd
4.36V
D
A1b
pd
pd
4.36V


A
5.8V
4.3V
B
5.8V
4.3V
C
5.8V
4.3V
D
5.8V
4.3V

Supplementary Files

This is a list of supplementary files associated with this preprint. Click to download.

- Supplementarytablesfinal.xlsx
- Fig.S3.png
- Fig.S1.png
- Fig.S4.png
- Fig.S2.png